

Hemispheric asymmetries in the ionospheric response observed in the American sector during an intense geomagnetic storm

A. J. de Abreu,¹ P. R. Fagundes,¹ Y. Sahai,¹ R. de Jesus,¹ J. A. Bittencourt,² C. Brunini,³ M. Gende,³ V. G. Pillat,¹ W. L. C. Lima,⁴ J. R. Abalde,¹ and A. A. Pimenta²

Received 11 May 2010; revised 2 August 2010; accepted 10 August 2010; published 10 December 2010.

[1] The main purpose of this investigation is to study the ionospheric F region response induced by the intense geomagnetic storm that occurred on 7–8 September 2002. The geomagnetic index Dst reached a minimum of -181 nT at 0100 UT on 8 September. In this study, we used observations from a chain of 12 GPS stations and another chain of 6 digital ionosonde stations. It should be mentioned that, soon after the sudden commencement (SC) at 1637 UT on 7 September, the TEC variations at midlatitude stations in both hemispheres showed an F region positive storm phase. However, during the recovery phase, a strong hemispheric asymmetry was observed in the ionospheric response. While a TID type soliton was observed to propagate in the Southern American sector, no TID activity was seen in the Northern American sector. Also, in the Southern Hemisphere, the TEC variations were less affected by the geomagnetic storm. The Northern Hemisphere observations showed a strong and long-lasting negative F region storm phase starting at about 1000 UT on 8 September (lasting for about 24 h). A perusal of TEC phase fluctuations and equatorial spread-F (ESF) ionospheric sounding data indicates that, on the disturbed night of 7–8 September, some stations showed the occurrence of ESF starting at about 0000 UT (2000 LT) on 8 September, whereas other stations showed that the ESF occurrence started much later, at about 0800 UT (0500 LT). This hemispheric asymmetric response of the ionospheric F region possibly indicates the presence of different mechanisms for the generation of ESF along the various latitudinal regions during the disturbed period.

Citation: de Abreu, A. J., et al. (2010), Hemispheric asymmetries in the ionospheric response observed in the American sector during an intense geomagnetic storm, *J. Geophys. Res.*, *115*, A12312, doi:10.1029/2010JA015661.

1. Introduction

[2] Studies related to space weather in the Sun–Earth system are of growing importance nowadays. F region ionospheric storms, induced by geomagnetic storms, represent an extreme form of space weather that can have significant and adverse effects on increasingly sophisticated ground- and space-based technological systems [Buonsanto, 1999; Jansen and Pirjola, 2004]. When the ionospheric electron density increases as a result of an ionospheric storm, the event is called a positive ionospheric storm or positive phase, while if a decrease in electron density is observed, the event is called a negative ionospheric storm or negative

phase [Prölss, 1993; Schunk and Sojka, 1996; Bauske and Prölss, 1998; Werner et al., 1999; Prölss and Werner, 2002]. As mentioned by Tsurutani et al. [2004] and Basu et al. [2007] drastic changes in the low-latitude ionosphere can be produced by intense disturbance electric fields originating from magnetosphere-ionosphere interaction. These electric fields are identified as prompt equatorward penetration of magnetospheric/high-latitude electric fields and may be also influenced by the global thermospheric wind circulation generated by Joule heating in the high-latitude atmosphere in consequence of particles precipitation [Abdu, 1997]. The electric fields, depending on their polarity and duration, can cause large upward or downward drifts of the ionospheric plasma [Tsurutani et al., 2004].

[3] Other possible sources of ionospheric perturbations are related to large-scale traveling ionospheric disturbances (TIDs). Joule heating generated by geomagnetic storms, at high latitudes, can produce traveling atmospheric disturbances (TADs). These TADs can interact with the ionosphere and produce large-scale TIDs with long horizontal wavelengths that travel equatorward with high speeds [Hines and Hooke, 1970; Killeen et al., 1984; Fagundes et al., 1995; Bauske and Prölss, 1998; Werner et al., 1999; Lima

¹Física e Astronomia, Universidade do Vale do Paraíba (UNIVAP), São José dos Campos, Brazil.

²Instituto Nacional de Pesquisas Espaciais (INPE), São José dos Campos, Brazil.

³Facultad de Ciencias Astronómicas y Geofísicas, Universidad Nacional de La Plata, La Plata, Argentina.

⁴Centro Universitário Luterano de Palmas, Universidade Luterana do Brasil, Palmas, Brazil.

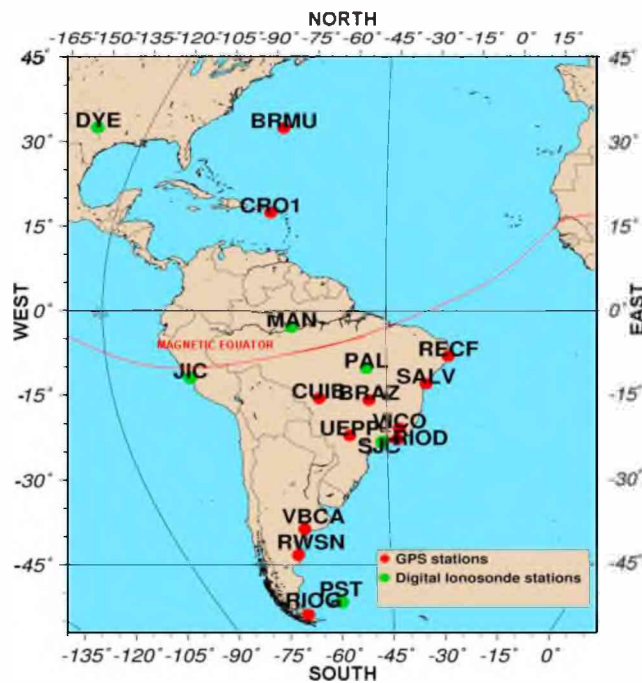


Figure 1. A map showing the locations of the GPS and digital ionosonde stations used in the present study. Also, the geographic and magnetic equators are shown.

et al., 2004; *Becker-Guedes et al.*, 2007]. Other important storm aspects are related to generation/suppression of equatorial ionospheric irregularities or equatorial spread-F (ESF) in the equatorial and low-latitude regions [*Whalen*, 2002; *Becker-Guedes et al.*, 2004; *Martinis et al.*, 2005; *Sahai et al.*, 2005, 2007, 2009a, 2009b, 2009c; *Fagundes et al.*, 2008, 2009a, 2009b; *de Jesus et al.*, 2010; *de Abreu et al.*, 2010].

[4] In this paper, we present and discuss the interhemisphere asymmetric response of the ionospheric F region induced by an intense geomagnetic storm that occurred on 7–8 September 2002. The interhemisphere and different longitudinal sector ionosphere responses to geomagnetic storms have been studied by *Blagoveshchensky et al.* [2003], *Sahai et al.* [2005], *Huang and Yumoto* [2006], *Karpachev et al.* [2007], and *Astafyeva* [2009]. *Astafyeva* [2009] using data of satellite altimeters Jason-1 and TOPEX (in different longitudinal sectors), and measurements from GPS receivers on-board CHAMP and SAC-C satellites (in different range of altitudes), observed a north–south asymmetry in the dayside redistribution of ionospheric plasma during an intense geomagnetic storm. *Sahai et al.* [2009b] using data from several GPS receiving stations in mid to low-equatorial regions in both hemispheres in the Latin American sector during the intense geomagnetic disturbances in the early part of November 2004, observed an asymmetry in the positive–negative storm phases. The data analyzed in this investigation cover observations from equatorial to midlatitudes over the American sector in both northern and southern American hemispheres. However, as far as we know, this is the first time that a TID soliton is

observed in the southern American hemisphere and no TID activity was seen in the Northern American sector.

[5] Observation of total electron content (TEC) and ionospheric parameters ($h'F$, foF_2 , presence of spread-F on ionograms) were conducted using 12 GPS and 6 ionosonde stations, respectively. This observation clearly shows the importance of using a ground-based chain of different instruments to study the ionospheric response to geomagnetic storms.

2. Observations

[6] The Global Positioning System (GPS) data used here were obtained in the standard format known as “Receiver Independent Exchange format (RINEX)” for the 12 receiving stations. Figure 1 and Table 1 provide full details of the GPS sites used in the present study. The GPS observations were used to obtain the vertical total electron content (VTEC, hereafter TEC), that is calculated in units of TEC (1 TEC unit = 10^{16} electrons/m²) [*Wanninger*, 1993] and the phase fluctuations (rate of change of TEC) is calculated in terms of TEC/min [*Aarons et al.*, 1996]. The Recife (RECF), Salvador (SALV), Cuiabá (CUIB), Brasília (BRAZ), Viçosa (VICO), Presidente Prudente (UEPP), and Rio de Janeiro (RIOD) stations belong to the “Rede Brasileira de Monitoramento Contínuo” (RBMC), or Brazilian Network for Continuous GPS Monitoring, operated by the “Instituto Brasileiro de Geografia e Estatística” (IBGE), or Brazilian Institute of Geography and Statistics. The Bahia Blanca (VBCA) and Rawson (RWSN) stations are operated through the “Servizo Argentino de GNSS” (SAG; Argentinian Service of GNSS). The Bermuda, United Kingdom (BRMU), St. Croix, U. S. Virgin Islands (CRO1), and Rio Grande (RIOG) stations belong to the International GNSS Service (IGS) for Geodynamics [*Dow et al.*, 2005]. All these stations are located in the American sector from equatorial region to midlatitudes in both hemispheres.

[7] Figure 1 and Table 1 provide full details of the ionosonde sites used in the present study. The ionospheric sounding stations at Manaus (MAN), Palmas (PAL), and São José dos Campos (SJC), Brazil, are equipped with the Canadian Advanced Digital Ionosonde (CADI) [*Grant et al.*, 1995; *Fagundes et al.*, 2008]. The ionospheric sounding stations Dyess AFB (DYE), USA, Jicamarca (JIC), Peru, and Port Stanley (PST) are equipped with the Digisonde Portable Sounder (DPS). The ionosondes were used to obtain ionospheric parameter variations, such as: F-layer minimum virtual height ($h'F$) and F-layer critical frequency (foF_2). A peculiarity exists for ionosondes installed in the equatorial region at MAN and PAL, due to the fact that both are located in southern geographic tropical region, but are in opposite hemispheres with respect to the magnetic equator (see Figure 1). Note that the ionosonde at MAN is located between the geographic and magnetic equators (see Figure 1). Also, the ionosonde located at JIC is almost at the magnetic equator. The ionosonde installed in SJC is near the southern crest of the equatorial ionospheric anomaly and the ionosonde installed in PST is located at midlatitude in the Southern Hemisphere.

[8] The geomagnetic indices Dst and AE were obtained from the Website <http://swdcwww.kugi.kyoto-u.ac.jp>. The geomagnetic index Kp was obtained from the Website <http://>

Table 1. Details of the GPS and Digital Ionosonde Sites Used in the Present Study

Location (Symbol)	Instrument	Coordinates	Dip Latitude	Local Time
Bermuda (BRMU)	GPS	32.4° N, 64.7° W	39.4° N	UT-4 h
St. Croix (CRO1)	GPS	17.4° N, 64.3° W	25.4° N	UT-4 h
Recife (RECF)	GPS	8.1° S, 35.0° W	13.1° S	UT-3 h
Salvador (SALV)	GPS	13.0° S, 38.5° W	15.16° S	UT-3 h
Cuiabá (CUIB)	GPS	15.6° S, 56.1° W	7.15° S	UT-4 h
Brasília (BRAZ)	GPS	15.9° S, 47.9° W	11.7° S	UT-3 h
Viçosa (VICO)	GPS	20.8° S, 42.9° W	18.6° S	UT-3 h
P. Prudente (UEPP)	GPS	22.1° S, 51.4° W	14.9° S	UT-3 h
R. de Janeiro (RIOD)	GPS	22.8° S, 43.3° W	19.8° S	UT-3 h
Bahia Blanca (VBCA)	GPS	38.7° S, 62.3° W	22.4° S	UT-4 h
Rawson (RWSN)	GPS	43.3° S, 65.1° W	24.7° S	UT-4 h
Rio Grande (RIOG)	GPS	53.8° S, 67.8° W	30.6° S	UT-4 h
Dye AFB (DYE)	DI	32.4° N, 99.8° W	42.4° N	UT-4 h
Manaus (MAN)	DI	2.9° S, 60.0° W	6.4° N	UT-4 h
Jicamarca (JIC)	DI	12.0° S, 76.8° W	0.05° S	UT-5 h
Palmas (PAL)	DI	10.2° S, 48.2° W	5.7° S	UT-3 h
S. J. dos Campos (SJC)	DI	23.2° S, 45.9° W	17.6° S	UT-3 h
Port Stanley (PST)	DI	51.6° S, 57.9° W	29.9° S	UT-4 h

ftp.gwdg.de/pub/geophys/kp-ap/tab/. The Bz-component of the interplanetary magnetic field (IMF) in geocentric solar magnetospheric (GSM) coordinates, the solar wind speed, and the solar wind ion density were obtained from the Website <http://www.srl.caltech.edu/ace/>.

3. Results and Discussions

[9] Figure 2 shows the time variations of the solar, interplanetary, and geomagnetic indices for the period studied (6–9 September 2002). The yellow and blue background portions highlight the solar-interplanetary-geomagnetic index variations during the geomagnetic storm main and recovery phases, respectively. Also, the black vertical arrow indicates the sudden commencement (SC). The sudden commencement (SC) started at 1637 UT on 7 September (see Figure 2). At the same time, the IMF-Bz turns southward to a value around -28 nT and there is an abrupt simultaneous increase in solar wind speed from about 400 km/s to about 580 km/s and ion density from about 5 cm $^{-3}$ to about 20 cm $^{-3}$, indicating the arrival of an interplanetary shock structure

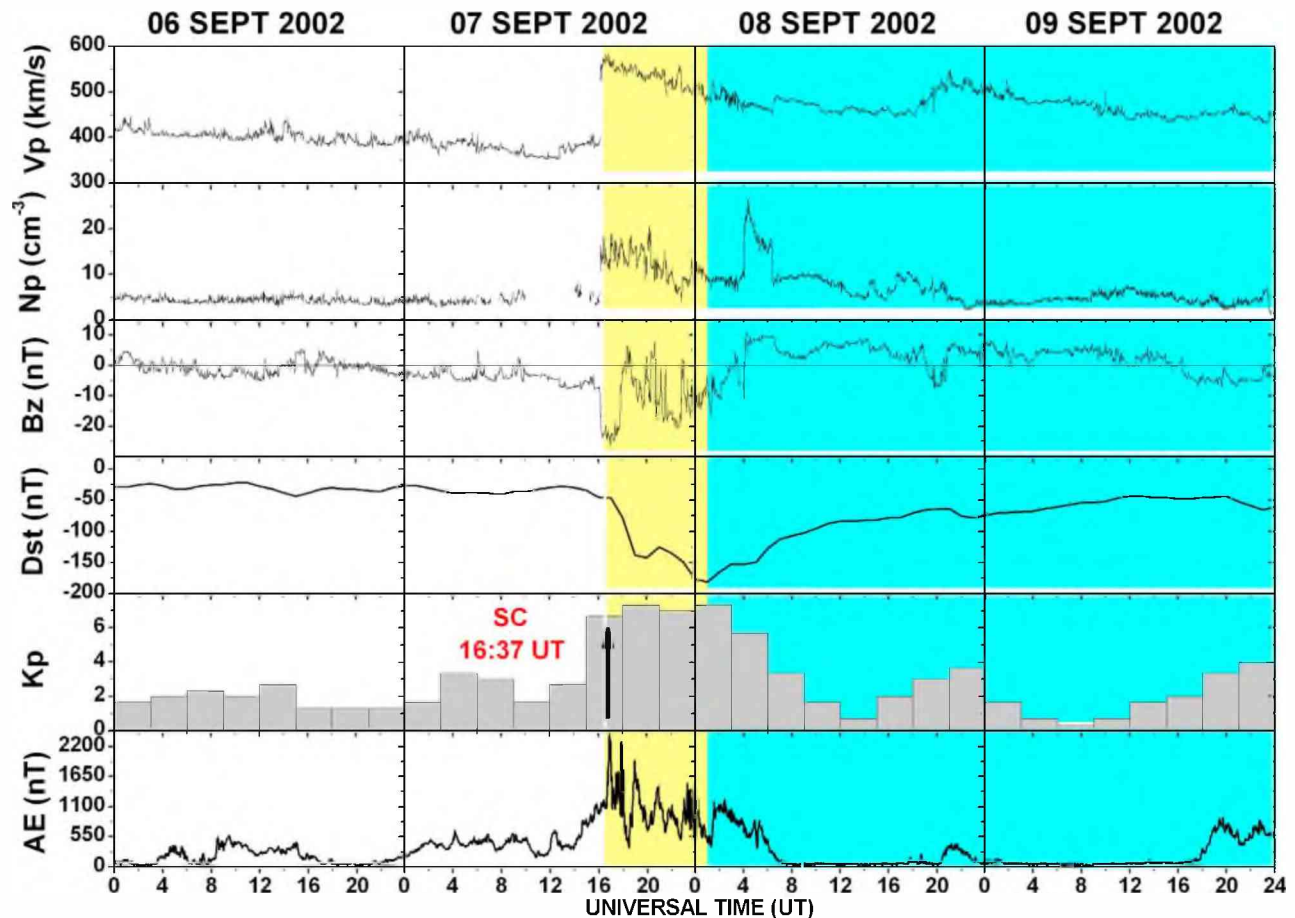


Figure 2. Variations of the solar wind proton bulk velocity V_p , solar wind ion density N_p , Bz component of IMF in the GSM coordinates, and geomagnetic indices Dst, Kp, and AE for the period 6–9 September 2002. The black vertical arrow indicates the sudden commencement (SC). The yellow and blue background portions highlight the geomagnetic main and recovery phases, respectively.

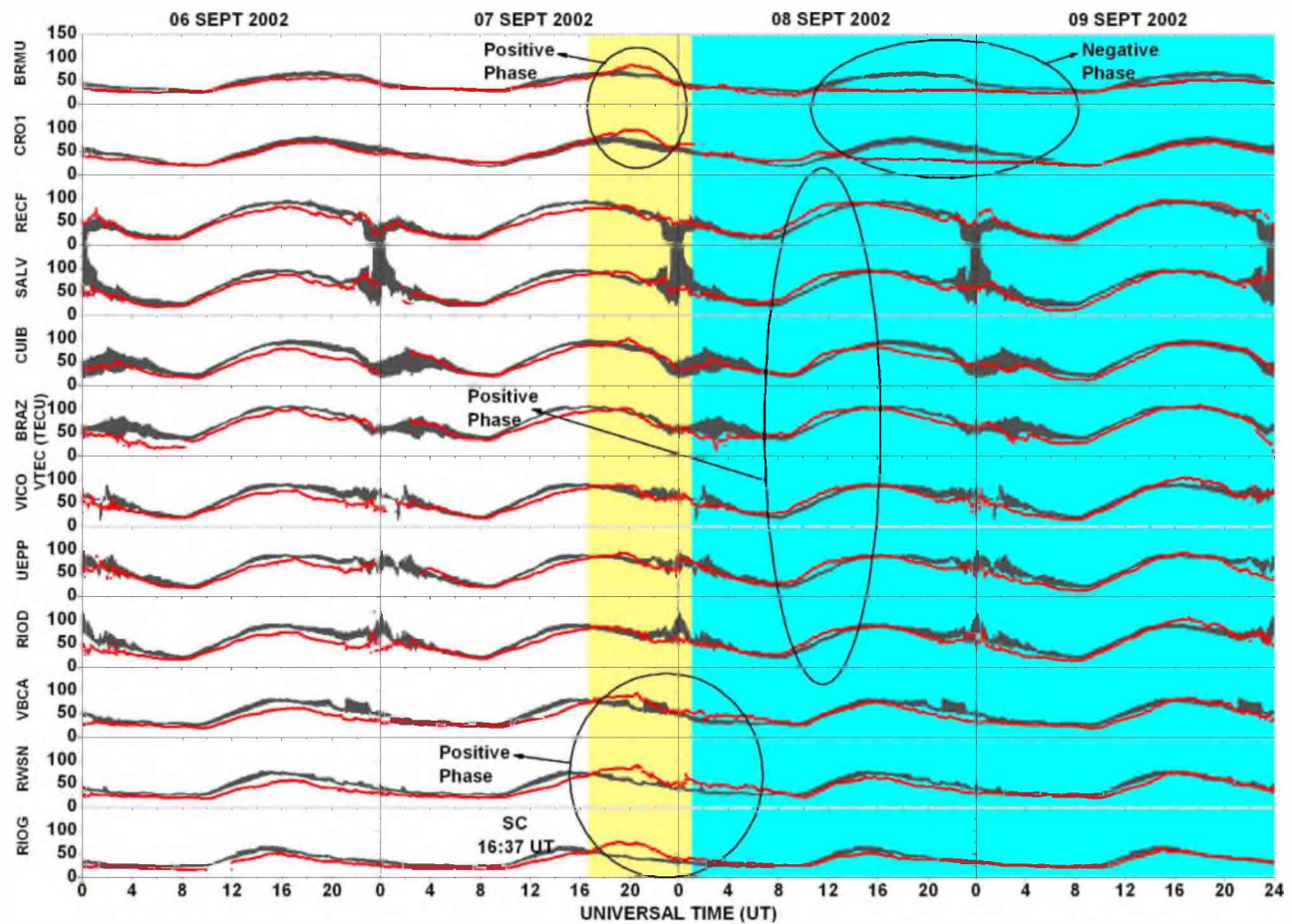


Figure 3. Variations of the vertical total electron content (VTEC) from GPS observations obtained from different satellites at 12 receiving stations during the period 6–9 September 2002 (red lines). The black bands are ± 1 standard deviation of the average quiet day (four quiet days) values.

leading to the formation of an intense geomagnetic storm. After the SC, during the storm main phase, the Kp index reached 7+ on the night of 7–8 September and the Dst index started decreasing from -47 nT at 1700 UT on 7 September, reaching -181 nT at 0100 UT on 8 September. As pointed out by *Basu et al.* [2001] and *de Abreu et al.* [2010], when rapid changes of the Dst index occur during the main storm phase, prompt penetration of magnetospheric electric field affects the ionospheric dynamics at low latitudes. At 0400 UT on 8 September, during the recovery storm phase, a new abrupt increase in ion density, from about 10 cm^{-3} to about 25 cm^{-3} was observed (Figure 2). At the same time, the IMF-Bz turns northward. Figure 2 also shows strong fluctuations in the AE index between about 1637 UT and 2400 UT on 7 September, indicating energy injection (substorm activity) at auroral latitudes due the Joule heating. As discussed out by *Kosch and Nielsen* [1995], the average ionospheric Joule heating appears to be linearly related with the increase of the AE index. As pointed out by numerous authors, this additional energy can launch a TAD and its interaction with the ionosphere can generate large-scale TIDs [*Crowley and Williams*, 1987; *Lima et al.*, 2004].

[10] Figure 3 shows the average vertical total electron content (TEC) variations obtained at 12 GPS receiving stations. The TEC values, for each station, were calculated using only satellites that have elevation angles larger than 30° . The observed TEC variations during the disturbed period are shown in red full line. The TEC averaged quiet period (four quiet days viz. 16, 17, 18, and 19 September) variations are shown as black bands and their widths correspond to ± 1 standard deviation. The yellow and blue background portions highlight the geomagnetic main and recovery phases, respectively.

[11] The ionospheric parameters foF2 and h'F daily variations are shown in Figures 4 and 5, respectively. The first panel shows the data observed at DYE, the second to fifth panels show the data observed at MAN, JIC, PAL, and SJC, respectively, and the last panel shows the data observed at PST. The ionospheric parameters (foF2 and h'F) observed during the disturbed period were obtained every 15 min from the ionograms, except at PST, in which they were obtained every 30 min (red line). The averaged foF2 and h'F (four quiet days viz. 16, 17, 18, and 19 September) variations are shown as black bands and their widths correspond to ± 1 standard deviation. Figure 5 also shows the horizontal

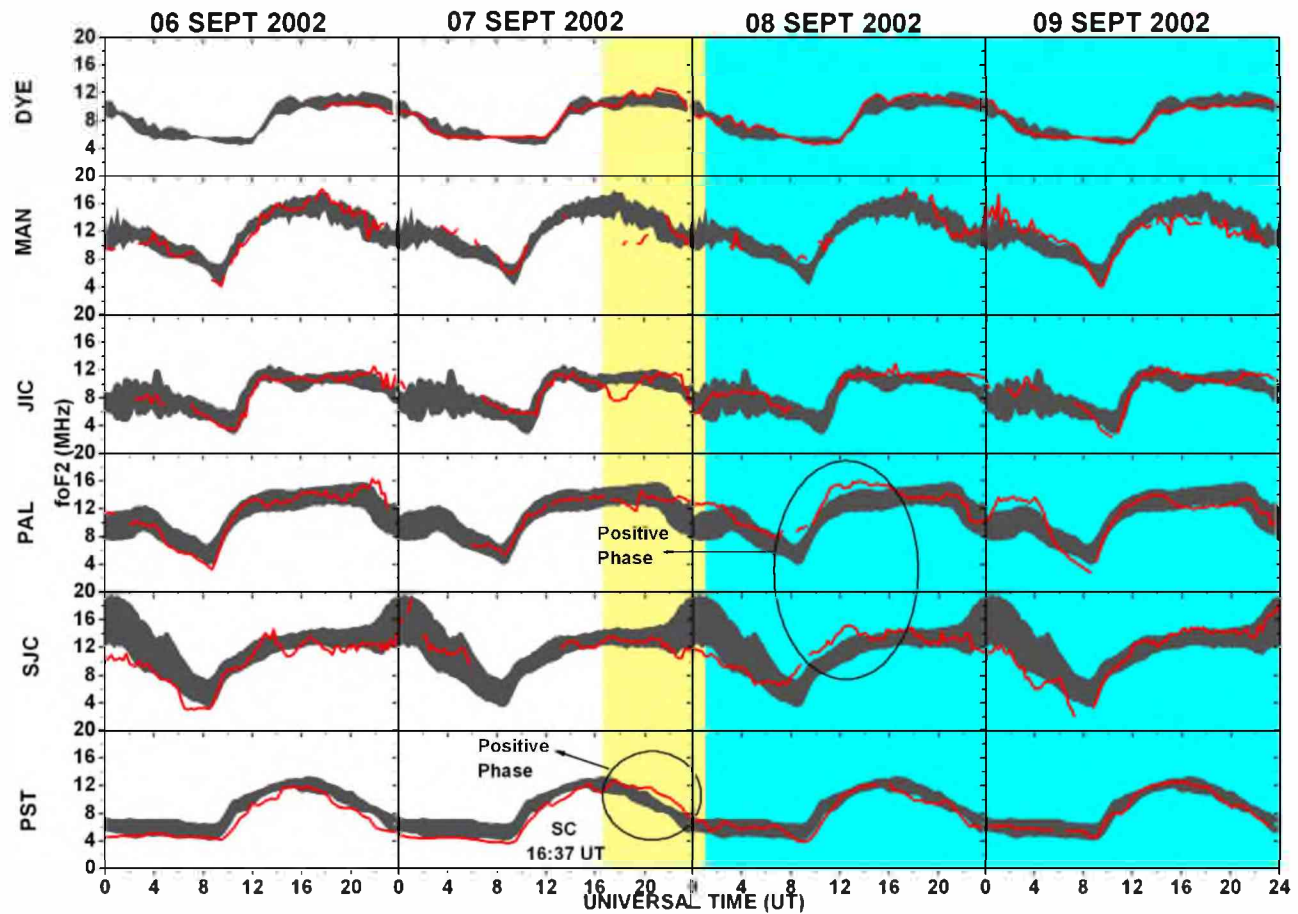


Figure 4. Variations of the ionospheric parameter foF2 obtained at Dyess AFB (DYE), Manaus (MAN), Jicamarca (JIC), Palmas (PAL), São José dos Campos (SJC), and Port Stanley (PST) during the period 6–9 September 2002 (red lines). The black bands are ± 1 standard deviation of the average quiet day values. The yellow and blue background portions highlight the geomagnetic main and recovery phases, respectively.

black bars indicating the equatorial spread-F (ESF). The yellow and blue background portions highlight the geomagnetic main and recovery phases, respectively.

3.1. Storm Main Phase

[12] A perusal of the TEC data (Figure 3) during the main phase shows a positive storm phase at midlatitudes in both hemispheres (North and South America). In the Northern Hemisphere, the positive storm phase was noted, at BRMU and CRO1 between about 1800 UT and 2200 UT, just after the SC, but it lasted only during the main phase. The foF2 (Figure 4) observed at DYE (midlatitude in Northern Hemisphere) did not show any significant change, in comparison to quiet days. This difference in behavior for the TEC and foF2 values is probably related to local variations, since the GPS stations and the ionosonde station are separated by about 35° in longitude. However, a positive storm phase in TEC in the Southern Hemisphere was noticed at RIOG, RWSN, and VBCA, but took place during the main phase and first 5 h of the recovery phase (see Figure 3). At the same time, a positive storm phase was observed in the ionospheric F region critical frequency (foF2) at the PST station (Figure 4). According *Werner et al.* [1999], travel-

ing atmospheric disturbances and changes in the large-scale wind circulation are more likely explanations for the observed positive ionospheric phase. Therefore, this positive ionospheric phase may be related to the TID soliton observed in the Southern Hemisphere (see Figure 5).

[13] Also, during the main phase, the TEC values at low latitudes and equatorial regions were not disturbed by the geomagnetic storm. Nevertheless, the foF2 values, at equatorial region, showed a very short negative phase (see Figure 4, JIC). This indicates that there was some redistribution in the vertical electron density profile that generated a very short negative storm phase in foF2, but did not affect the TEC values.

3.2. Storm Recovery Phase

[14] During the recovery phase the TEC in the Northern Hemisphere midlatitude stations showed a strong and long-lasting negative storm phase (BRMU and CRO1) (see Figure 3). Also, it is possible to notice that foF2 at DYE (a midlatitude station in North America) had a daily time variation similar to quiet days. This difference in behavior between TEC and foF2 is probably associated with local variations, since the GPS stations and ionosonde station are

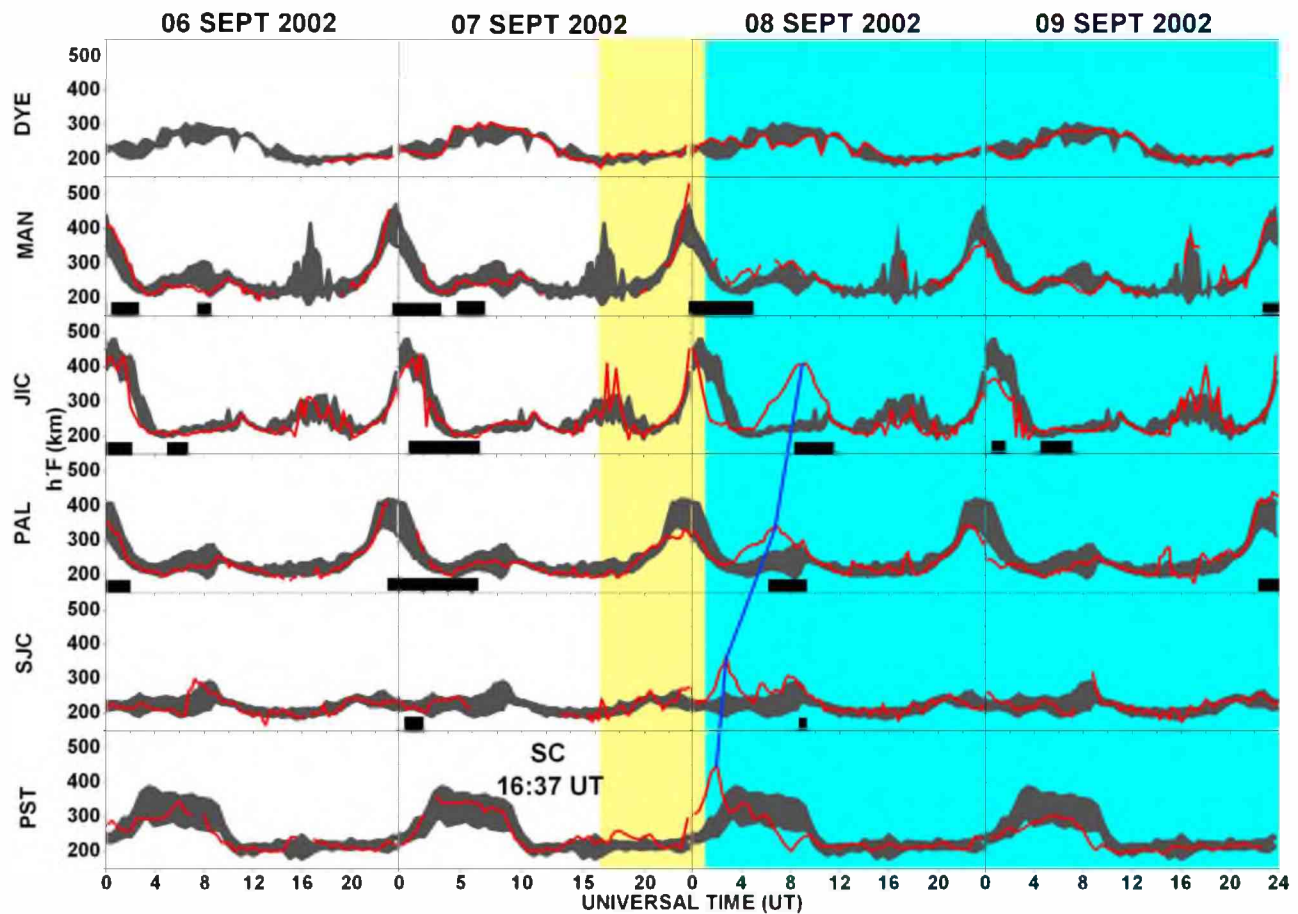


Figure 5. Variations of the ionospheric parameter $h'F$ obtained at Dyess AFB (DYE), Manaus (MAN), Jicamarca (JIC), Palmas (PAL), São José dos Campos (SJC), and Port Stanley (PST) during the period 6–9 September 2002 (red lines). The black bands are ± 1 standard deviation of the average quiet day values. Also, the horizontal black bars indicate the presence of equatorial spread-F (ESF). The yellow and blue background portions highlight the geomagnetic main and recovery phases, respectively.

well separated in longitude. The long negative storm phase observed in the Northern Hemisphere is possibly associated with an O/N_2 density ratio decrease [Danilov and Morozova, 1985; Pröls and Werner, 2002].

[15] On the other hand, the TEC in the midlatitude Southern Hemisphere (VBCA, RWSN, and RIOG), during the recovery phase, presented most of the time, a quiet day behavior. Also, there is a weak TEC positive storm phase at low and equatorial regions (RECF to RIOD) during the recovery phase (8 September). The same positive storm phase observed on TEC, at low latitude, is also observed from the ionospheric sounding (foF_2) at PAL and SJC. Probably, the observed positive phase (Southern Hemisphere) is related to the passage of the TID soliton during the recovering phase at equatorial and low latitudes. As mentioned by Bauske and Pröls [1998], the winds are more important for ionospheric positive storm phase effect than neutral composition changes. Also, Werner *et al.* [1999] showed that composition changes (perturbations of the O/N_2 density ratio) are not sufficient to explain the storm effects and traveling atmospheric disturbances. Changes in the large-scale wind circulation are a more likely explanation for the observed positive ionospheric phase. On the other hand,

the negative phase can almost entirely be explained by neutral gas composition changes [Pröls and Werner, 2002; Pröls, 2003].

[16] Finally, during the last day of the recovery phase (9 September 2002) the TEC values from midlatitude to equatorial regions return to its quiet-day variations. Therefore, the data clearly shows that there is a hemisphere asymmetry in TEC response during the recovery phase at midlatitudes.

3.3. Traveling Ionospheric Disturbance Type Soliton

[17] Figure 5 shows the virtual height ($h'F$) daily variations for the period 6–9 September 2002. The ionospheric parameter data covers a wide latitude range from North to South American hemispheres (DYE, MAN, JIC, PAL, SJC, and PST).

[18] One of the most interesting features observed in the $h'F$ parameter behavior, during disturbed period, is a TID soliton propagating from midlatitude to the equatorial region in Southern Hemisphere. The $h'F$ maximum values were observed at PST (midlatitude), SJC (low latitude), PAL (near equatorial region) and JIC (equatorial region) at approximately 0200 UT, 0245 UT, 0645 UT, and 0915 UT,

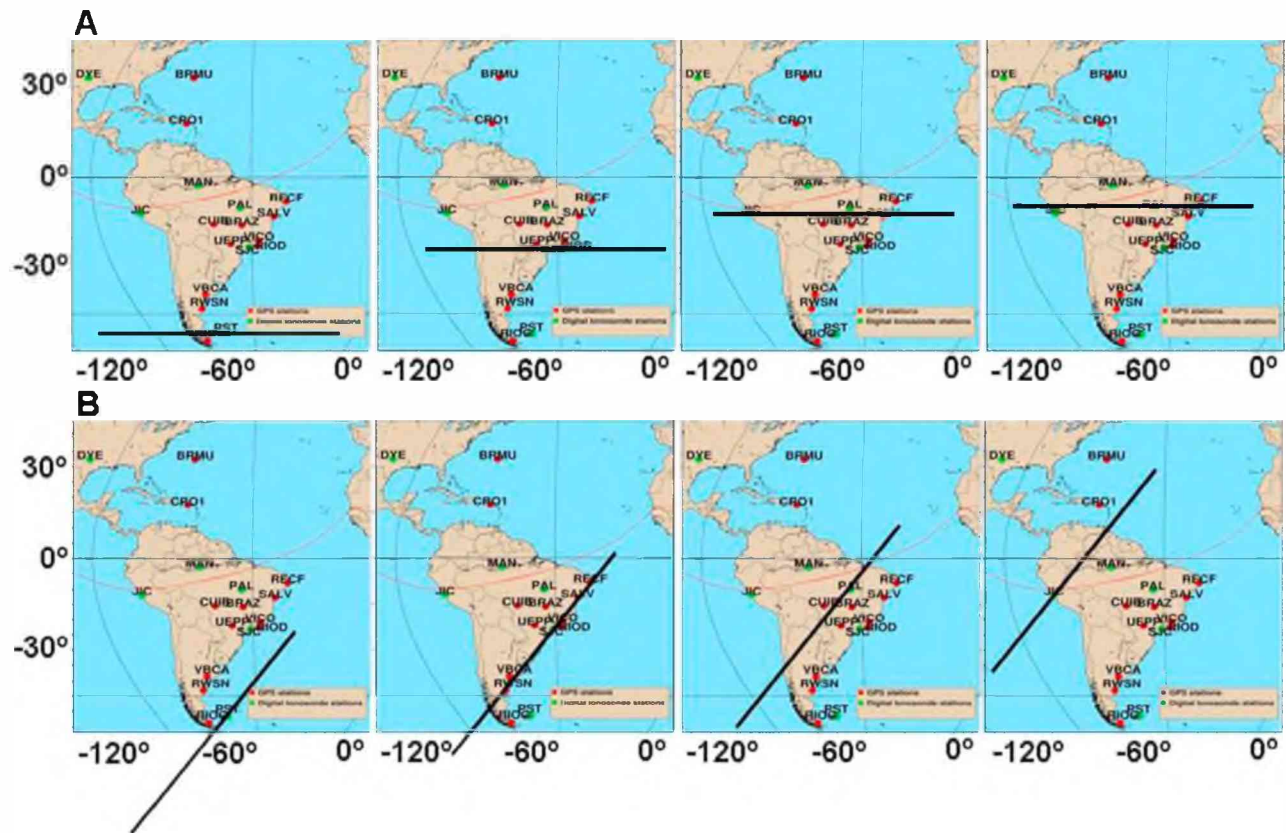


Figure 6. (a) A sequence of maps showing the TID type soliton propagating only in the northward direction. (b) A sequence of 4 maps showing the TID type soliton propagating in the northwest direction. In both cases TID type soliton is represented by a thick black line.

respectively. In Figure 5, a blue full line links the observed TID peaks, in order to highlight the wave propagation characteristics.

[19] It appears that this TID soliton was generated at high latitudes during the main phase (7 September) and propagated toward the equatorial region. It reached the low latitude and equatorial region during the recovery phase (8 September). Notice that the TID soliton, after traveling a few thousands kilometers, arrived at the equatorial region broader than it was originally observed at midlatitude. On the other hand, this peak was not present at the MAN station, suggesting that the TID soliton propagated only in the southern magnetic hemisphere.

[20] If we were to assume that the TID soliton propagated only northward (shown by the black thick line in Figure 6a), then there appears at least two significant inconsistencies in the analysis. There are strong discrepancies between the velocities from midlatitude to low latitude (PST to SJC ~ 1000 m/s) and from low-latitude to equatorial regions (SJC to PAL ~ 100 m/s). A velocity of about 1000 m/s is too high, when compared to values obtained by other investigators [Fagundes *et al.*, 1995; Lee *et al.*, 2002; Lima *et al.*, 2004]. Also, we do not expect that the TID velocity changed that much during its motion from midlatitude to equator regions.

[21] Also, if we assume that TID soliton propagated only northward, the TID soliton should arrive almost simulta-

neously at PAL and JIC, but first at PAL and just a little bit later at JIC, since, JIC is located at 12.0° S and PAL at 10.2° S. The observations show exactly the contrary, i.e., the TID soliton arrives first at PAL and only 2:45 h later it arrives at JIC. The long time lag between JIC and PAL (2:45 h) suggested that the TID soliton has a zonal component propagation. If we assume that the TID soliton travels to the northwest direction, toward the sunset sector (shown by the black thick line in Figure 6b). Then, the TID soliton has zonal and meridional velocity components.

[22] Then, just tilting the propagation direction, it is possible to solve the problem of high-speed velocity inferred from PST to SJC and the time lag between PAL and JIC. Now, the two inconsistencies mentioned above are solved. Then the TID soliton travels with a velocity of about 100 to 300 m/s and arrives first at PAL and afterward at JIC.

[23] On the other hand, the $h'f$ values at the DYE station did not show any TID activity. This indicates that the ionospheric response to the geomagnetic storm was different in the Northern and Southern Hemispheres, in spite of the fact that we should expected similar ionosphere responses in both hemispheres during the equinox month of September. However, since there is a separation between the geographic and magnetic equators in this longitudinal region, and since the ionospheric dynamics is somewhat controlled by the

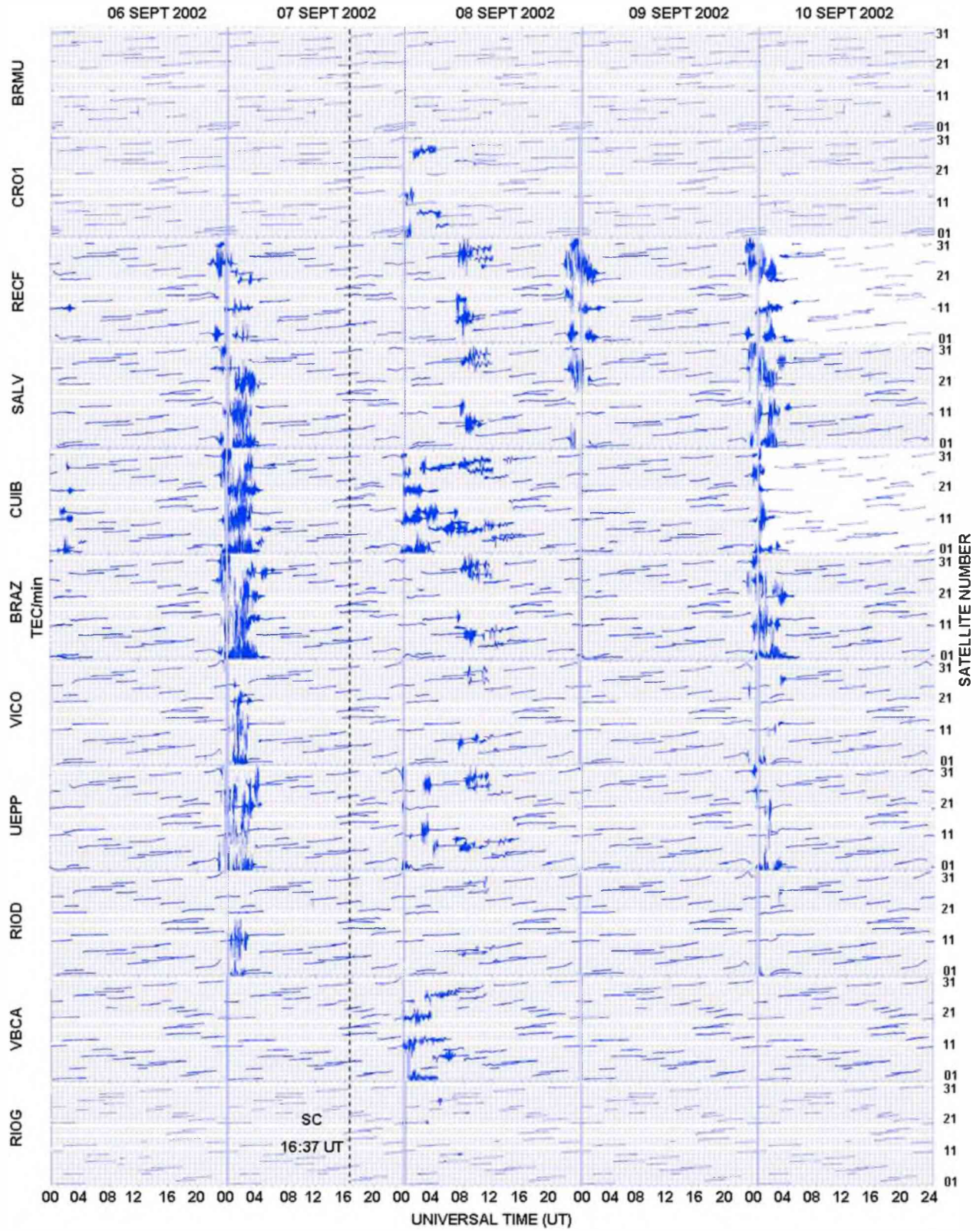


Figure 7. The phase fluctuations (rate of change of TEC) from GPS observations obtained from different satellites at 12 receiving stations during the period 6–10 September 2002. The black vertical dashed line indicates the time of sudden commencement (SC).

magnetic field, some asymmetric behavior is expected to occur, even during equinox months.

3.4. Ionospheric Irregularities

[24] Figure 7 shows the TEC phase fluctuations (rate of change of TEC) for the period of 6–10 September 2002 and the black vertical dashed line indicates the sudden commencement (SC). As pointed out by Aarons *et al.* [1997], the TEC phase fluctuations indicate the presence of ionospheric irregularities with size of the order of kilometers.

[25] It is noted that on 6–7 September (a quiet night) and 9–10 September (the last night of the recovery phase) the presence of equatorial ionospheric irregularities from equator to low-latitude stations (RECF to RIOD; Figure 7). Note that the irregularities appear around 2300 UT (2000 LT), first in the near equatorial region (see RECF station), and subsequently (starting around 2400 UT; 2100 LT) they are observed at higher latitude stations (see e.g., VICO and UEPP stations). This is a classical picture that we expect from large-scale equatorial ionospheric irregularities or plasma bubbles, since these irregularities extend from equatorial to low latitude (in both hemispheres). The extension of the irregularity toward low latitudes will depend on the height; the large-scale irregularity reaches in the equatorial region [Otsuka *et al.*, 2002].

[26] However, on the night of 7–8 September, during the end of main phase and first day of the recovery phase, the irregularities are present at mid to low-equatorial latitudes in the Southern Hemisphere at different times (Figure 7). The most peculiar feature of this night is the complete asynchronism of the irregularities onset time. The observed features are possibly caused by a combination of the post sunset electric field prereversal enhancement at equatorial region that generates the large-scale spread-F and by the passage of TID soliton that uplift the bottomside of the *F* region and creating favorable condition for spread-F generation at midlatitude and equatorial region.

[27] Apparently, only the equatorial Brazilian west side (MAN, Figure 5) had large-scale spread-F generated by the *F*-layer rapid postsunset uplift caused by electric field prereversal enhancement. Also, see phase fluctuations at CUIB and UEPP (Figure 7). The *h'**F* at MAN and PAL (Figure 5) reinforce this idea, because the postsunset *F*-layer uplift was stronger at MAN (Brazilian west side) and weaker at PAL (Central part of Brazil), suggesting again that there is latitudinal gradient on the *F*-layer rapid postsunset up-lift.

[28] Since the central and east Brazilian side did not have strong post sunset prereversal enhancement on this night. Therefore, there was no formation of equatorial spread-F in this sector. However, the TID soliton front is considered tilted and it reaches first the equatorial Brazilian east side (see Figure 6b). This result in a rapid uplift of *F* region bottom side and creates conditions for generation of spread-F. The TEC phase fluctuation can be seen at RECF, SALV, BRAZ, and VICO (Figure 7).

[29] On the other hand, there are TEC phase fluctuations at midlatitude stations (Figure 7; VBCA and RWSN, Argentina). These TEC phase fluctuations indicate the presence of irregularities and these irregularities coincide with the passage of the TID type soliton at these sites. Then, probably the irregularities generated were caused by the passage of the TID soliton. The *F*-layer was uplifted by the TID soliton

creating favorable conditions for generation of spread-F, via Perkins instability [Pimenta *et al.*, 2008].

4. Conclusions

[30] In this paper we have presented and analyzed ionospheric data from 12 GPS receiver stations located from Bermuda (32.4° N, 64.7° W) to Rio Grande (53.8° S, 67.8° W), as well as ionospheric sounding data obtained at Dyess AFB (32.4° N, 99.8° W), USA, to Port Stanley (51.6° S, 57.9° W) in mid to low-equatorial regions in the American sector, during the intense geomagnetic storm of 7–9 September 2002. Some of the salient features related to these observations and analysis are summarized below.

[31] During the main phase there is a positive storm phase in both midlatitude American hemispheres. Also, during the recovery phase, the northern American sector at midlatitudes showed a strong and long-lasting negative storm phase, while southern American sector, at midlatitudes, presented a quiet-day behavior.

[32] The *h'**F* variations suggested that a TID soliton was generated at high southern latitudes, during the main phase, and reached midlatitudes, during the recovery phase. Also, the event time sequence observed at different ionosonde sites suggests that a TID traveled toward northwest direction. As far as we know, this is the first time that the direction of the TID was inferred by a chain of ionosondes.

[33] On 7 September 2002 (recovery phase), spread-F was generated by a rapid post-sunset *F*-layer uplift (Brazilian west sector) and the *F*-layer uplift caused by the TID type soliton (midlatitude and Brazilian east sector).

[34] **Acknowledgments.** Thanks are due to the Brazilian funding agencies for the partial financial support through grants 08/05482-5 (FAPESP), 301469/2009-1 and 555307/2008-5 (CNPq). The JIC, DYE, and PST data were obtained from the Digital Ionogram DataBase (DIDBase) (Bodo Reinisch). The Jicamarca Radio Observatory is a facility of the Instituto Geofísico del Perú operated with support from the NSF Cooperative Agreement ATM-0432565 through Cornell University.

[35] Robert Lysak thanks the reviewers for their assistance in evaluating this paper.

References

- Aarons, J., M. Mendillo, R. Yantosca, and E. Kudeki (1996), GPS phase fluctuations in the equatorial region during the MISETA 1994 campaign, *J. Geophys. Res.*, *101*(A12), 26,851–26,862, doi:10.1029/96JA00981.
- Aarons, J., M. Mendillo, and R. Yantosca (1997), GPS phase fluctuations in the equatorial region during sunspot minimum, *Radio Sci.*, *32*, 1535–1550, doi:10.1029/97RS00664.
- Abdu, M. A. (1997), Major phenomena of the equatorial ionosphere-thermosphere system under disturbed conditions, *J. Atmos. Sol. Terr. Phys.*, *59*(13), 1505–1519, doi:10.1016/S1364-6826(96)00152-6.
- Astafyeva, E. I. (2009), Dayside ionospheric uplift during strong geomagnetic storms as detected by the CHAMP, SAC-C, TOPEX and Jason-1 satellites, *Adv. Space Res.*, *43*, 1749–1756, doi:10.1016/j.asr.2008.09.036.
- Basu, S., et al. (2001), Ionospheric effects of major magnetic storms during the International Space Weather Period of September and October 1999: GPS observations, VHF/UHF scintillations, and in situ density structures at middle and equatorial latitudes, *J. Geophys. Res.*, *106*(A12), 30,389–30,413, doi:10.1029/2001JA001116.
- Basu, S., et al. (2007), Response of the equatorial ionosphere at dusk to penetration electric fields during intense magnetic storms, *J. Geophys. Res.*, *112*, A08308, doi:10.1029/2006JA012192.
- Bauske, R., and G. W. Pröls (1998), Numerical simulation of long-duration positive ionospheric storm effects, *Adv. Space Res.*, *22*(1), 117–121, doi:10.1016/S0273-1177(97)01110-1.
- Becker-Guedes, F., Y. Sahai, P. R. Fagundes, W. L. C. Lima, V. G. Pillat, J. R. Abalde, and J. A. Bittencourt (2004), Geomagnetic storm and equa-

- torial spread-F, *Ann. Geophys.*, *22*(9), 3231–3239, doi:10.5194/angeo-22-3231-2004.
- Becker-Guedes, F., et al. (2007), The ionospheric response in the Brazilian sector during the super geomagnetic storm on 20 November 2003, *Ann. Geophys.*, *25*(4), 863–873, doi:10.5194/angeo-25-863-2007.
- Blagoveshchensky, D. V., O. M. Pirog, N. M. Polekn, and L. V. Chistyakova (2003), Mid-latitude effects of the May 15, 1997 magnetic storm, *J. Atmos. Sol. Terr. Phys.*, *65*, 203–210, doi:10.1016/S1364-6826(02)00227-4.
- Buonsanto, M. J. (1999), Ionospheric storms—A review, *Space Sci. Rev.*, *88*, 563–601, doi:10.1023/A:1005107532631.
- Crowley, G., and P. J. S. Williams (1987), Observation of the source and propagation of atmospheric gravity waves, *Nature*, *328*, 231–233, doi:10.1038/328231a0.
- Danilov, A. D., and L. D. Morozova (1985), Ionospheric storms in the F2 region—Morphology and physics (review), *Geomagn. Aeron.*, *25*, 593–605.
- de Abreu, A. J., Y. Sahai, P. R. Fagundes, F. Becker-Guedes, R. de Jesus, F. L. Guarnieri, and V. G. Pillat (2010), Response of the ionospheric F region in the Brazilian sector during the super geomagnetic storm in April 2000 observed by GPS, *Adv. Space Res.*, *45*, 1322–1329, doi:10.1016/j.asr.2010.02.003.
- de Jesus, R., et al. (2010), Effects observed in the ionospheric F region in the South American sector during the intense geomagnetic storm of 14 December 2006, *Adv. Space Res.*, doi:10.1016/j.asr.2010.04.031.
- Dow, J. M., R. E. Neilan, and G. Gendt (2005), The International GPS Service (IGS): Celebrating the 10th anniversary and looking to the next decade, *Adv. Space Res.*, *36*(3), 320–326, doi:10.1016/j.asr.2005.05.125.
- Fagundes, P. R., A. L. Aruliah, D. Rees, and J. A. Bittencourt (1995), Gravity-wave generation and propagation during geomagnetic storms over Kiruna (67.8° N, 20.4° E), *Ann. Geophys.*, *13*(4), 358–366, doi:10.1007/s00585-995-0358-7.
- Fagundes, P. R., M. T. A. H. Muella, J. A. Bittencourt, Y. Sahai, W. L. C. Lima, F. L. Guarnieri, F. Becker-Guedes, V. G. Pillat, A. S. Ferreira, and N. S. Lima (2008), Nighttime ionosphere-thermosphere coupling observed during an intense geomagnetic storm, *Adv. Space Res.*, *41*, 539–547, doi:10.1016/j.asr.2007.11.005.
- Fagundes, P. R., J. A. Bittencourt, J. R. Abalde, Y. Sahai, M. J. A. Bolzan, V. G. Pillat, and W. L. C. Lima (2009a), F Layer postsunset height rise due to electric field preversal enhancement: 1. Traveling planetary wave ionospheric disturbance effects, *J. Geophys. Res.*, *114*, A12321, doi:10.1029/2009JA014390.
- Fagundes, P. R., J. R. Abalde, J. A. Bittencourt, Y. Sahai, R. G. Francisco, V. G. Pillat, and W. L. C. Lima (2009b), F layer postsunset height rise due to electric field preversal enhancement: 2. Traveling planetary wave ionospheric disturbances and their role on the generation of equatorial spread F, *J. Geophys. Res.*, *114*, A12322, doi:10.1029/2009JA014482.
- Grant, I. F., J. W. McDougall, J. M. Ruohoniemi, W. A. Bristow, G. J. Sofko, J. A. Koehler, D. Danskin, and D. Andre (1995), Comparison of plasma flow velocities determined by the ionosonde Doppler drift technique, SuperDARN radars, and patch motion, *Radio Sci.*, *30*, 1537–1549, doi:10.1029/95RS00831.
- Hines, C. O., and W. H. Hooke (1970), Discussion of ionization effects on the propagation of acoustic-gravity waves in the ionosphere, *J. Geophys. Res.*, *75*, 2563–2568, doi:10.1029/JA075i013p02563.
- Huang, C.-S., and K. Yumoto (2006), Quantification and hemispheric asymmetric of low-latitude geomagnetic disturbances caused by solar wind pressure enhancements, *J. Geophys. Res.*, *111*, A09316, doi:10.1029/2006JA011831.
- Jansen, F., and R. Pirola (2004), Space weather research elucidates risks to technological infrastructure, *Eos Trans. AGU*, *85*(25), 241–245.
- Karpachev, A. T., L. Z. Biktash, and T. Maruyama (2007), The high-latitude ionosphere structure on 22 March, 1979 magnetic storm from multi-satellite and ground-based observation, *Adv. Space Res.*, *40*, 1852–1857, doi:10.1016/j.asr.2007.04.088.
- Killeen, T. J., P. B. Hays, G. R. Carignan, R. A. Heelis, W. B. Hanson, N. W. Spencer, and L. H. Brace (1984), Ion-neutral coupling in the high-latitude F region: Evaluation of ion heating terms from Dynamics Explorer 2, *J. Geophys. Res.*, *89*, 7495–7508.
- Kosch, M. J., and E. Nielsen (1995), Coherent radar estimates of average high-latitude ionospheric Joule heating, *J. Geophys. Res.*, *100*(A7), 12,201–12,215.
- Lee, C. C., J. Y. Liu, B. W. Reinisch, Y. P. Lee, and L. B. Liu (2002), The propagation of traveling atmospheric disturbances observed during the April 6–7, 2000 ionospheric storm, *Geophys. Res. Lett.*, *29*(5), 1068, doi:10.1029/2001GL013516.
- Lima, W. L. C., F. Becker-Guedes, Y. Sahai, P. R. Fagundes, J. R. Abalde, G. Growley, and J. A. Bittencourt (2004), Response of the equatorial and low-latitude ionosphere during the space weather events of April 2002, *Ann. Geophys.*, *22*, 3211–3219, doi:10.5194/angeo-22-3211-2004.
- Martinić, C. R., M. J. Mendillo, and J. Aarons (2005), Toward a synthesis of equatorial spread F onset and suppression during geomagnetic storms, *J. Geophys. Res.*, *110*, A07306, doi:10.1029/2003JA010362.
- Otsuka, Y., K. Shiokawa, T. Ogawa, and P. Wilkinson (2002), Geomagnetic conjugate observations of equatorial airglow depletions, *Geophys. Res. Lett.*, *29*(15), 1753, doi:10.1029/2002GL015347.
- Pimenta, A. A., M. C. Kelley, Y. Sahai, J. A. Bittencourt, and P. R. Fagundes (2008), Thermospheric dark band structures observed in all-sky OI 630 nm emission images over the Brazilian low-latitude sector, *J. Geophys. Res.*, *113*, A01307, doi:10.1029/2007JA012444.
- Pröls, G. W. (1993), On explaining the local time variation of ionospheric storm effects, *Ann. Geophys.*, *11*, 1–9.
- Pröls, G. W. (2003), *Physics of the Earth's Space Environment: An Introduction*, Springer, New York.
- Pröls, G. W., and S. Werner (2002), Vibrationally excited nitrogen and oxygen and the origin of negative ionospheric storms, *J. Geophys. Res.*, *107*(A2), 1016, doi:10.1029/2001JA900126.
- Sahai, Y., et al. (2005), Effects of the major geomagnetic storms of October 2003 on the equatorial and low-latitude F region in two longitudinal sectors, *J. Geophys. Res.*, *110*, A12S91, doi:10.1029/2004JA010999.
- Sahai, Y., et al. (2007), Response of nighttime equatorial and low latitude F region to the geomagnetic storm of August 18, 2003, in the Brazilian sector, *Adv. Space Res.*, *39*(8), 1325–1334, doi:10.1016/j.asr.2007.02.064.
- Sahai, Y., et al. (2009a), Observations of the F region ionospheric irregularities in the South American sector during the October 2003 'Halloween Storms', *Ann. Geophys.*, *27*(12), 4463–4477, doi:10.5194/angeo-27-4463-2009.
- Sahai, Y., et al. (2009b), Effects observed in the Latin American sector ionospheric F region during the intense geomagnetic disturbances in the early part of November 2004, *J. Geophys. Res.*, *114*, A00A19, doi:10.1029/2007JA013007.
- Sahai, Y., et al. (2009c), Effects observed in the ionospheric F region in the east Asian sector during the intense geomagnetic disturbances in the early part of November 2004, *J. Geophys. Res.*, *114*, A00A18, doi:10.1029/2008JA013053.
- Schunk, R. W., and J. J. Sojka (1996), Ionosphere-thermosphere space weather issues, *J. Atmos. Terr. Phys.*, *58*(14), 1527–1574, doi:10.1016/0021-9169(96)00029-3.
- Tsurutani, B. T., et al. (2004), Global dayside ionospheric uplift and enhancement associated with interplanetary electric fields, *J. Geophys. Res.*, *109*, A08302, doi:10.1029/2003JA010342.
- Wanninger, L. (1993), Effects of the Equatorial Ionosphere on GPS, *GPS World*, *4*, 48–54.
- Werner, S., R. Bauske, and G. W. Pröls (1999), On the origin of positive ionospheric storms, *Adv. Space Res.*, *24*(11), 1485–1489, doi:10.1016/S0273-1177(99)00711-5.
- Whalen, J. A. (2002), Dependence of equatorial bubbles and bottomside spread F on season, magnetic activity, and $E \times B$ drift velocity during solar maximum, *J. Geophys. Res.*, *107*(A2), 1024, doi:10.1029/2001JA000039.

J. R. Abalde, A. J. de Abreu, R. de Jesus, P. R. Fagundes, V. G. Pillat, and Y. Sahai, Física e Astronomia, Universidade do Vale do Paraíba, São José dos Campos, São Paulo 12244, Brazil. (abreu.alessandro@gmail.com)
 J. A. Bittencourt and A. A. Pimenta, Instituto Nacional de Pesquisas Espaciais, São José dos Campos, São Paulo 12201-970, Brazil.
 C. Brunini and M. Gende, Facultad de Ciencias Astronómicas y Geofísicas, Universidad Nacional de La Plata, La Plata 1900, Argentina.
 W. L. C. Lima, Centro Universitário Luterano de Palmas, Universidade Luterana do Brasil, Palmas, Tocantins 77054-970, Brazil.